

# Radiographic Evaluation of Osteochondral Defect Repair using a Tissue-Engineered Scaffold with and without Bone Marrow Mesenchymal Stem Cells in Rabbits

Mursaleen Rashid<sup>1</sup>, Shahid Hussain Dar<sup>2</sup>, Mudasir Bashir Gugjoo<sup>2\*</sup>, Showkat Ahmad Shah<sup>3</sup>, Amatul Muhee<sup>2</sup>

## ABSTRACT

The regeneration of osteochondral defects remains a major clinical challenge due to the limited regenerative capacity of articular cartilage and the structural complexity of the osteochondral unit. Simultaneous regeneration of cartilage and subchondral bone with seamless integration at their interface is required for the effective repair. The current study was carried out to develop and evaluate an effective tissue engineered scaffold with or without bone marrow mesenchymal stem cells (BM-MSC) for regeneration of osteochondral defects. An *in vivo* study was carried out in New Zealand white rabbits (n=24) randomly distributed into 3 groups as per the treatment protocol. Standardized osteochondral defects were created in the trochlear groove of the left distal femur. The radiographic evaluation on day 45 post surgery revealed moderate increase in radiopacity in both groups II and III, while substantial increase in defect radiopacity was seen at day 90. At day 90 radiographic characteristics had improved compared to day 45 in test scaffold as well as BM-MSC seeded scaffold group animals compared to the untreated group animals. Radiographic evaluation corroborated these findings, demonstrating progressive defect filling, restoration of surface contour, and gradual mineralization of subchondral bone without pathological changes. These findings suggest that the developed scaffold, particularly when combined with BM-MSCs, effectively supports osteochondral regeneration.

**Key words:** Bone marrow MS cells, Osteochondral defect, Rabbit, Scaffold.

*Ind J Vet Sci and Biotech* (2026); 10.48165/ijvsbt.22.2.34

## INTRODUCTION

Osteoarthritis is a chronic, progressive disorder that significantly impairs mobility, causes persistent pain, and diminishes quality of life (Lou *et al.*, 2025; Tang *et al.*, 2025). Once regarded as a simple degenerative condition, it is now recognized as a multifactorial disease affecting the entire joint complex, including cartilage, bone, ligaments, and surrounding musculature (Tang *et al.*, 2025). Osteochondral defects remain particularly challenging due to the limited intrinsic repair capacity of cartilage, which lacks vascular, neural, and lymphatic networks, and the complex architecture of articular cartilage and subchondral bone (Lin *et al.*, 2022; Dai *et al.*, 2023). Despite the availability of conventional treatments such as microfracture, autologous cell transplantation and osteochondral grafting, long term outcomes are often compromised by inadequate regeneration and graft failure (Arden *et al.*, 2021; Dai *et al.*, 2023; Lou *et al.*, 2025). Scaffold-based tissue engineering has emerged as a promising strategy, employing biphasic, triphasic, and multiphasic scaffolds to replicate native tissue organisation and demonstrated superior performance compared to single-phase designs; however, their regenerative potential in relation to natural concentration gradients and layer orientation remains insufficiently explored (Gugjoo *et al.*,

<sup>1</sup>Division of Veterinary Surgery & Radiology, Faculty of Veterinary Sciences and Animal Husbandry, Shuhama, SKUAST-K, Sringar-190006, Kashmir, India

<sup>2</sup>Division of Veterinary Clinical Complex, Faculty of Veterinary Sciences and Animal Husbandry, Shuhama, SKUAST-K, Sringar-190006, Kashmir, India

<sup>3</sup>Division of Veterinary Pathology, Faculty of Veterinary Sciences and Animal Husbandry, Shuhama, SKUAST-K, Sringar-190006, Kashmir, India

**Corresponding Author:** Dr. Mudasir Bashir Gugjoo, Assistant Professor, Division of Veterinary Clinical Complex, Faculty of Veterinary Sciences and Animal Husbandry, Shuhama, SKUAST-K, Sringar-190006, Kashmir, India. e-mail: mbgugjoo@gmail.com

**How to cite this article:** Rashid, M., Dar, S. H., Gugjoo, M. B., Shah, S. A., & Muhee, A. (2026). Radiographic Evaluation of Osteochondral Defect Repair using a Tissue-Engineered Scaffold with and without Bone Marrow Mesenchymal Stem Cells in Rabbits. *Ind J Vet Sci and Biotech*, 22(2), 178-181.

**Source of support:** Nil

**Conflict of interest:** None

**Submitted** 12/01/2026 **Accepted** 08/02/2026 **Published** 10/03/2026

2020; Zhou *et al.*, 2022; Nikhil *et al.*, 2024). Building on this gap, the present study was aimed to evaluate an osteochondral scaffold designed to mimic the composition and layered

architecture of natural cartilage, using radiographic parameters to assess defect healing and mineralization in a rabbit model.

## MATERIALS AND METHODS

### Experimental Animals

The study was carried out at Stem cell lab, Division of Veterinary Clinical Complex and Division of Veterinary Surgery & Radiology, Faculty of Veterinary Sciences and Animal Husbandry, Shuhama, SKUAST-K, Sringar-190006, Kashmir, India from May, 2025 to September, 2025 following approval of IAEC (FVSc/IAEC/2025/22). A total of 24 clinically healthy New Zealand white rabbits (*Oryctolagus cuniculus*), average age of 3 months and weighing 2.6 kg were subjected to thorough physical and clinical examination before creation of osteochondral defect. The animals were randomly allocated into three experimental groups (n=8 per group), viz., Group I: Untreated control (defect left empty), Group II: Osteochondral defect treated with test scaffold, and Group III: Osteochondral defect treated with BM-MSC-seeded scaffold. All experimental procedures were conducted following institutional ethical guidelines for animal experimentation.

### Surgical Creation of Osteochondral Defect

The surgical site was aseptically prepared and anaesthesia was induced using combination of Xylazine HCl (8 mg/kg, IM) and followed 10 min later by Ketamine HCl (80 mg/kg, IM). A standardized osteochondral defect measuring 4×4 mm was created in the middle of the trochlear groove at non-weight bearing surface of the left knee joint using a manually operated drill. Haemostasis was achieved by gentle blotting to prevent hematoma formation prior to scaffold implantation. The surgical procedures were carried in strict aseptic conditions. In group I, defect was left empty with no scaffold implanted. In Group II, test scaffolds were implanted into the defect, and test scaffold seeded with BM-MSCs were implanted into the group III animals. After implantation, patella was relocated and the joint capsule, subcutaneous tissue followed by skin were routinely closed using vicryl 2-0 suture material after 10 min of scaffold implantation.

### Postoperative Care

Regular antiseptic dressings were performed for 7 days post operatively and antibiotics and analgesics were injected for 7 days and 3 days, respectively. Animals were allowed free cage activity post-operatively and monitored daily for signs of pain, lameness, or wound complications.

### Radiographic Evaluation

For evaluating the defect healing at 0, 45, and 90 days post-surgery, standardized radiographic parameters of 40 kVp, 8 mAs, and a film-focus distance (FFD) of 75 cm were used. Radiographs were obtained in extended limb position using an anteroposterior projection. All radiographs were

subsequently digitized, and quantification of radiopacity values using ImageJ software was performed.

### Statistical Analysis

Data were expressed as mean  $\pm$  standard deviation (SD). One-way analysis of variance followed by Tukey's *post hoc* test was used for intergroup comparisons at days 45 and 90. Within-group comparisons were performed using Student's *t*-test. Statistical significance was set at  $p < 0.05$  and  $p < 0.01$ .

## RESULTS AND DISCUSSION

At day 0, radiographs revealed sharp demarcation of defect margins with minimal radiopacity, consistent with untreated osteochondral damage. In the untreated control group (Group I), the defect remained clearly visible at day 45 with negligible mineralization and unchanged defect diameter. By day 90, persistent radiolucency with irregular margins was observed, indicating limited spontaneous repair. These findings corroborated with previous reports demonstrating that untreated osteochondral defects typically heal poorly and are often filled with fibrocartilaginous tissue rather than hyaline cartilage (Gugjoo *et al.*, 2020; Tortorici *et al.*, 2021; Voltres-Martínez *et al.*, 2025). The untreated group served as a critical control, highlighting the necessity of scaffold-based interventions to stimulate cellular activity, matrix deposition and defect integration and validates the therapeutic potential of tissue engineered biomaterials.

In group II, radiographs immediately following implantation of the test scaffold showed distinct defect margins with minimal internal radiopacity. By day 45, moderate increase in radiopacity within the defect was apparent suggesting early mineral deposition and scaffold-mediated osteogenesis. The defect margins appeared less defined, indicating partial integration with surrounding bone. These findings are consistent with the results reporting scaffold's role in promoting cellular infiltration and matrix deposition using bioactive multilayered constructs (Zhang *et al.*, 2021; Tamaddon *et al.*, 2022). By day 90, substantial radiopacity was observed throughout the defect, with restoration of joint surface continuity and indistinguishable boundaries between the scaffold region and native bone. Increased trabecular formation and improved superficial cortical architecture were evident compared to the untreated group, confirming the osteoconductive and osteoinductive properties of the scaffold.

In Group III, radiographic findings were comparable to Group II at early stages, but demonstrated superior healing at later time points. By day 45, moderate radiopacity and early mineralization were observed, consistent with scaffold-mediated osteogenesis enhanced by BM-MSC activity. At day 90, radiographs revealed near-complete defect filling, dense trabecular organization, and seamless integration with adjacent bone. Radio dense lines extending toward the articular surface suggested advanced

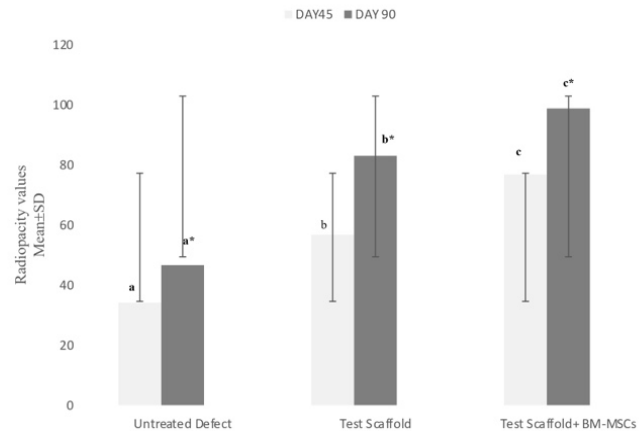


Figure 1: Anteroposterior radiographs of the stifle joint were obtained to evaluate osteochondral defect repair at predetermined time intervals. The defects were surgically induced in the trochlear groove of the left femur in New Zealand White rabbits. Radiographic exposure parameters were set at 50kVp and 8mAs with film-focus distance of 75cm. Radiographic assessment demonstrated superior defect healing in groups treated with Test scaffold + BM-MSCs followed by Test Scaffold and Untreated defect. Radiopacity values of the repaired defects were quantified using image analysis software at 45 and 90 days post surgical treatment. Different superscript letters (a, b, c) indicate significant intergroup differences ( $p < 0.05$ ) - indicates significant difference within the same group ( $p < 0.001$ )

subchondral bone regeneration and improved cartilage–bone interface restoration. These findings aligned with the known osteogenic and trophic effects of BM-MSCs, which promote extracellular matrix synthesis, angiogenesis, and long-term tissue remodelling (Gugjoo *et al.*, 2020; Nikhil *et al.*, 2024).

Quantitative radiopacity analysis further supported these observations, demonstrating significantly higher radiopacity values in both scaffold-treated groups compared to the untreated group, with the BM-MSC-seeded scaffold showing the greatest improvement. These results also aligned with previous studies reporting scaffold mediated repair of osteochondral defects (Tortorici *et al.*, 2021; Tamaddon *et al.*, 2022).

In conclusion, the study demonstrated that the tissue-engineered osteochondral scaffold effectively promotes repair of osteochondral defects, with enhanced outcomes observed when combined with BM-MSCs. Radiographic evidence confirmed progressive defect filling, subchondral bone mineralization, and improved structural integration over time. The findings support the potential of BM-MSC-seeded scaffolds as a promising strategy for osteochondral tissue regeneration.

## ACKNOWLEDGEMENT

The authors are highly thankful to the funding agencies including the SERB (EMR/2027/ 001484), DBT (BT/

PR46254//1/861/2022) and ANRF (ANRF/ARG/2025/000011/LS) to make this work possible.

## REFERENCES

- Arden, N.K., Perry, T.A., Bannuru, R.R., Bruyère, O., Cooper, C., Haugen, I.K., & Reginster, J.Y. (2021). Non-surgical management of knee osteoarthritis: Comparison of ESCO and OARSI 2019 guidelines. *National Reviews on Rheumatology* 17(1), 59–66.
- Dai, W., Cheng, J., Yan, W., Cao, C., Zhao, F., Li, Q., & Ao, Y. (2023). Enhanced osteochondral repair with hyaline cartilage formation using an extracellular matrix-inspired natural scaffold. *Science Bulletin*, 68(17), 1904–1917.
- Gugjoo, M.B., Amarpal, Abdelbaset-Ismail, A., Aithal, H.P., Kinjavdekar, P., Kumar, G.S., & Sharma, G.T. (2020). Allogeneic mesenchymal stem cells and growth factors in gel scaffold repair osteochondral defects in rabbits. *Regenerative Medicine*, 15 (2), 1261–1275.
- Lin, C.Y., Wang, Y.L., Chen, Y.J., Ho, C.T., Chi, Y.H., Chan, L.Y., & Hung, S.C. (2022). Collagen-binding peptides for enhanced imaging, lubrication and regeneration of osteoarthritic cartilage. *Nature Biomedical Engineering*, 6(10), 1105–1117.
- Lou, W., Qiu, X., Qin, Y., Lu, Y., Cao, Y., & Lu, H. (2025). 3D-printed scaffold armed with skeletal stem cell-derived exosomes enhances osteochondral regeneration. *Bioactive Materials*, 51, 231–256.
- Nikhil, A., Gugjoo, M.B., Das, A., Manzoor, T., Ahmad, S.M., Ganai, N.A., & Kumar, A. (2024). Multilayered cryogel enriched with exosomes regenerates cartilage architecture in goat osteochondral injuries. *ACS Applied Materials & Interfaces*, 16(47), 64505–64521.



- Tamaddon, M., Blunn, G., Tan, R., Yang, P., Sun, X., Chen, S.M., & Liu, C. (2022). In vivo evaluation of additively manufactured multilayered scaffold for repair of large osteochondral defects. *Bio-Design and Manufacturing*, 5(3), 481-496.
- Tang, S.A., Zhang, C., Oo, W.M., Fu, K., Risberg, M.A., Bierma-Zeinstra, S.M., & Hunter, D.J. (2025). Osteoarthritis. *Nature Reviews Disease Primers*, 11(1), 1-22.
- Tortorici, M., Petersen, A., Ehrhart, K., Duda, G.N., & Checa, S. (2021). Scaffold-dependent mechanical and architectural cues guide osteochondral defect healing in silico. *Frontiers in Bioengineering and Biotechnology*, 9, 642217.
- Voltes-Martínez, A., Martínez-Moreno, D., Pleguezuelos-Beltrán, P., Nygren-Jiménez, E., Lopez-Ruiz, E., & Marchal, J.A. (2025). Advances in mimetic extracellular matrix-based biofabricated scaffolds enriched with hydroxyapatite for osteochondral regeneration. *Biofabrication*, 17(1), 012001.
- Zhou, H., Yuan, L., Xu, Z., Yi, X., Wu, X., Mu, C., & Li, D. (2022). Fabrication of heterogeneous three-layer scaffold mimicking osteochondral tissue. *ACS Applied BioMaterials*, 5(2), 734-746.